Atomistic locking and friction

Motohisa Hirano
Applied Electronics Laboratories, Nippon Telegraph and Telephone Corporation, Musashino, Tokyo 180, Japan

Kazumasa Shinjo
Basic Research Laboratories, Nippon Telegraph and Telephone Corporation, Musashino, Tokyo 180, Japan
(Received 26 October 1989; revised manuscript received 12 February 1990)

When solid bodies contact and slide against each other, the frictional phenomenon occurs. The origin of the related frictional force is studied by assuming the existence of two clean crystal surfaces, which follows the current experimental trends. This study theoretically clarifies the atomistic origin of the frictional force intrinsically generated by the molecular interactions between the constituent atoms of solids, but not the force extrinsically generated by surface asperities, the existence of foreign atoms, etc. Furthermore, this study assumes that the constituent atoms of the two contacting surfaces interact with each other due to the interaction potential. This study found that there are two origins: *atomistic locking* and *dynamic locking*. Atomistic locking occurs when the configuration of the atoms on a contact surface continuously changes with the sliding distance and when the interatomic potentials have an arbitrary strength. In contrast, dynamic locking occurs when the configuration discontinuously changes due to the dynamic process and if the interatomic potential is stronger than a specific given value. A criterion is derived for the occurrence of dynamic locking. From studying various systems, it can be seen that dynamic locking is unlikely to occur in realistic systems. The frictional forces due to atomistic locking are calculated for α-iron. One other important finding prior to the experiments is that certain unique cases exist where the frictional force exactly vanishes if completely clean solid surfaces are prepared.

I. INTRODUCTION

When two solid bodies contact each other and one body subsequently slides against the other, the frictional phenomenon occurs.[1] Enormous amounts of experimental data has shown that energy, i.e., frictional energy, is necessary for sliding contacting bodies. This indicates that a force (frictional force) parallel to the contacting interfaces appears.

Several models (or views) have been proposed to explain the origin of this frictional force. Some relate to the mechanical locking of surface asperities,[2] and others to the atomistic origin, i.e., the molecular interaction between the constituent atoms of solids.[3] A solution to the problems of coefficients of friction in real systems is achieved from the viewpoint of phenomenology by *a priori* assuming that the frictional force exists.[4] In real systems the data usually measured contain many unknown factors: surface roughness, poisoning by contaminants such as O_2, H_2, and oil, etc. It is difficult, therefore, to study the origin of the frictional force from the experiment data available at present. More recent experimental studies,[5,6] however, try to exclude many of the unknown factors by preparing well-defined surfaces. The purity and completion of such surfaces can be detected by current surface-analysis techniques such as scanning tunneling microscopy (STM).[7]

To understand the frictional-force mechanisms, this paper theoretically considers the atomistic origin of the frictional force on clean solid surfaces. It clarifies the origin of the frictional force that is generated by intrinsic factors, such as molecular interactions between constituent atoms, not by extrinsic factors such as surface asperities or surface contaminants. The system studied consists of two solid crystals: the upper and lower body. The lower body is assumed to be rigid, and the upper body slides against it. The atoms belonging to both bodies are assumed to interact with each other by pairwise interatomic potentials. The frictional properties are investigated for a quasistatic case where the upper body slides very slowly against the lower one. Atoms are considered to form the most favorable configuration by changing their positions during quasistatic sliding. Thus the concept of adiabatic potential is introduced to analyze the interaction energy operating between all the constituent atoms and the changes in their configurations. In general, the configuration of the atoms changes either continuously or discontinuously during sliding. The energy necessary for these configurations of the atoms to change is the frictional energy. This energy could dissipate into lattice vibrations, but the detailed mechanisms of such energy dissipation are not investigated here.

The organization of this paper is as follows. Section II defines the model for friction. The expressions for the adiabatic potential, frictional energy, and frictional force are obtained by assuming a rigid lower body. Section III examines an unrelaxed upper-body case, in which both of the upper and lower bodies are assumed to be rigid, by allowing the interplanar distance between the two bodies to vary during sliding. In this case, the configuration of the

atoms continuously changes, resulting in one atomistic origin called *atomistic locking*. Section IV analyzes a relaxed upper-body case, where the upper body is allowed to relax during sliding, in relation to the strength of the interaction potential existing between the two sliding bodies. In this case, the configuration of the atoms changes either continuously or discontinuously during sliding. The discontinuous change of the configuration results in the other atomistic origin called *dynamic locking*. In addition, friction transition is observed where frictional force changes from vanishing to finite as the interaction potential strengthens and a criterion for this occurrence is derived. Section V discusses the frictional properties of various systems in connection with the friction transition analyzed in Sec. IV.

II. THEORETICAL PRELIMINARIES

A. Adiabatic potential

The adiabatic potential is defined by the total energy when two contacting solid bodies slide against each other. This assumes that the upper body slides against a fixed lower body. It is also assumed that the upper body has N^u atoms and the lower body N^l atoms, and that the constituent atoms belong to both bodies interact with each other. The position coordinates of the atoms are denoted by $\mathbf{r}_i=(r_i^x,r_i^y,r_i^z)$ where $i=1,2,\ldots,(N^u+N^l)$. The total energy is a function of the position vectors $\mathbf{r}_i$ of all the atoms:

$$W(\mathbf{Q}:\{\mathbf{r}_i\}) . \tag{2.1}$$

$\mathbf{Q}$ stands for the displacement vector of the upper body against the lower body. An $\mathbf{r}_i$ coordinate set satisfies the relationship

$$\mathbf{Q}=\sum_i^{N^u}\mathbf{r}_i/N^u \quad \text{and} \quad \mathbf{0}=\sum_i^{N^l}\mathbf{r}_i/N^l . \tag{2.2}$$

Thus, the adiabatic potential spans a $3(N^u+N^l-1)$-dimensional potential surface. A set of $\mathbf{r}_i$ is determined so as to minimize $W(\mathbf{Q}:\{\mathbf{r}_i\})$ for a given $\mathbf{Q}$. The adiabatic potential can then be denoted as $W(\mathbf{Q})$, since $\mathbf{r}_i$ is a function of $\mathbf{Q}$. In general, the configuration of the atoms can change either continuously or discontinuously as $\mathbf{Q}$ varies.

Suppose $\mathbf{Q}$ and $\mathbf{Q}'$ are very close. Frictional energy $W(\mathbf{Q},\mathbf{Q}')$ is defined as the energy necessary for the configuration at $\mathbf{Q}'$ to change into the one at $\mathbf{Q}$. Thus, the frictional force $\mathbf{F}(\mathbf{Q})$ and the critical frictional force $\mathbf{F}_c$, which are required to slide two contacting bodies against each other, can be obtained by

$$\mathbf{F}(\mathbf{Q})=\lim_{\mathbf{Q}'\to\mathbf{Q}}\frac{W(\mathbf{Q},\mathbf{Q}')}{\mathbf{Q}-\mathbf{Q}'} , \tag{2.3}$$

and

$$\mathbf{F}_c=\text{maximum of } \mathbf{F}(\mathbf{Q}) . \tag{2.4}$$

Frictional energy $W(\mathbf{Q}_1,\mathbf{Q}_2)$ is lost along the path from $\mathbf{Q}_1$ to $\mathbf{Q}_2$ and can be obtained by

$$W(\mathbf{Q}_1,\mathbf{Q}_2)=\int_{\text{path}}-(d\mathbf{Q},\mathbf{F}(\mathbf{Q}))_i , \tag{2.5}$$

where $(\mathbf{x},\mathbf{y})_i$ stands for an inner product between vectors $\mathbf{x}$ and $\mathbf{y}$; this notation will be used throughout this paper. Frictional energy depends on the path. Average frictional force $F_{\text{av}}(\mathbf{Q}_1,\mathbf{Q}_2)$ along a path from $\mathbf{Q}_1$ to $\mathbf{Q}_2$ is

$$F_{\text{av}}(\mathbf{Q}_1,\mathbf{Q}_2)=\frac{W(\mathbf{Q}_1,\mathbf{Q}_2)}{\int_{\text{path}}|d\mathbf{Q}|} . \tag{2.6}$$

Equations (2.3)–(2.6) generally hold true when any two bodies slide against each other.

B. Model

The model involves two contacting surfaces that have some form of simple symmetry for simplification such as fcc (face-centered cubic), bcc (body-centered cubic), or hcp (hexagonal closed packed) lattices. Each atom belonging to the upper (or lower) body is denoted by a (or b):

$$V_{aa}(r), \quad V_{ab}(r), \quad \text{and} \quad V_{bb}(r) . \tag{2.7}$$

$V_{cd}(r)$ $(c,d=a \text{ or } b)$ describes the interaction between atoms c and d (r denotes the interatomic distance between two atoms). $V_{ab}(0)=0$ and $V_{aa}(0)=0$ are used throughout this paper. This assumption means the exclusion of the self-energy part of the interactions between constituent atoms from the expressions derived below. This is equivalent to $\sum'$, where the summation when $i=j$ in Eq. (2.8), for example, is excluded. The relative positions for the primitive vectors of the two contact surfaces are shown in Fig. 1. These primitive vectors are denoted by $\mathbf{g}_1'$, $\mathbf{g}_2'$, $\mathbf{g}_1$, and $\mathbf{g}_2$ and $\mathbf{q}_0$ is a misfit vector. The following section studies frictional properties for when an upper body moves quasistatically along a certain direction parallel to the contacting surface against a stationary lower body.

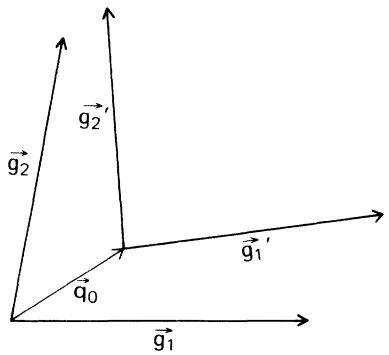

FIG. 1. General configuration where the primitive cell is spanned by primitive vectors: $\mathbf{g}_1'$ and $\mathbf{g}_2'$ of the upper body and contacts a primitive cell spanned by primitive vectors: $\mathbf{g}_1$ and $\mathbf{g}_2$ of the lower body with misfit vector q_0.

C. Expression for adiabatic potential

The adiabatic potential is obtained by

$$W(\mathbf{Q})=\sum_{i}^{N^u}\sum_{j}^{N^l}V_{ab}(|\mathbf{r}_i-\mathbf{r}_j|)+\tfrac{1}{2}\sum_{i,j}^{N^u,N^u}V_{aa}(|\mathbf{r}_i-\mathbf{r}_j|)\ . \tag{2.8}$$

Remember that $V_{ab}(0)=0$ and $V_{aa}(0)=0$. Here, the summation of j in the first term of the right-hand side is expressed by

$$V^l(r)=\sum_{j}^{N^l}V_{ab}(|\mathbf{r}-\mathbf{r}_j|)\ . \tag{2.9}$$

$V^l(r)$ is the interaction energy that the atoms of the upper body receive from the atoms of the lower body. The term $V_{bb}(|\mathbf{r}_i-\mathbf{r}_j|)$ is dropped, since it has no Q dependence. $V^l(r)$ has a periodicity characterized by the primitive vectors of the top layer of the lower body. Also, an upper body with a simple symmetry can be regarded as a stacked layered crystal. Equation (2.8) can be rewritten by making use of these facts.

A new notation $\mathbf{r}_i^\gamma$ or $(\boldsymbol{\rho}_i^\gamma,z_i^\gamma)$ is introduced, where $\boldsymbol{\rho}_i^\gamma$ stands for the components of the positional vectors on the γth layer, which is referenced by counting γ layers up from the bottom layer of the upper body. z_i^γ stands for the z components of the positional vectors on the γth layer. Notation $\mathbf{r}_i=(r_i^x,r_i^y,r_i^z)$ is still used in Sec. IV and positional vector $\mathbf{r}_i^\gamma$ can be expressed by using primitive vectors $\mathbf{g}_1$ and $\mathbf{g}_2$ of the lower body:

$$\mathbf{r}_i^\gamma=(\boldsymbol{\rho}_i^\gamma,z_i^\gamma)=(x_i^\gamma\mathbf{g}_1+y_i^\gamma\mathbf{g}_2+\Delta\boldsymbol{\rho}_i^\gamma,z_i^\gamma)\ . \tag{2.10}$$

Here, $\Delta\boldsymbol{\rho}_i^\gamma$ is defined by

$$\Delta\boldsymbol{\rho}_i^\gamma=\Delta x_i^\gamma\mathbf{g}_1+\Delta y_i^\gamma\mathbf{g}_2\quad(0\le\Delta x_i^\gamma,\Delta y_i^\gamma<1)\ . \tag{2.11}$$

x_i^γ and y_i^γ are integers that define $\Delta\boldsymbol{\rho}_i^\gamma$ in Eq. (2.11). x_i^γ, y_i^γ, Δx_i^γ, and Δy_i^γ are obtained from a given vector $\boldsymbol{\rho}_i^\gamma$ as

$$x_i^\gamma=[X_i^\gamma]\ \text{ and }\ y_i^\gamma=[Y_i^\gamma]\ , \tag{2.12}$$

and

$$\Delta x_i^\gamma=X_i^\gamma-[X_i^\gamma]\ \text{ and }\ \Delta y_i^\gamma-[Y_i^\gamma]\ . \tag{2.13}$$

X_i^γ and Y_i^γ are defined by

$$X_i^\gamma=\frac{(\boldsymbol{\rho}_i^\gamma,\mathbf{g}_1)_i}{|\mathbf{g}_1|}\ \text{ and }\ Y_i^\gamma=\frac{(\boldsymbol{\rho}_i^\gamma,\mathbf{g}_2)_i}{|\mathbf{g}_2|}\ , \tag{2.14}$$

where $[x]$ is Gauss notation and stands for a maximum integer that is equal to or smaller than x. Accordingly, Eq. (2.8) is rewritten as

$$W(\mathbf{Q})=\int d\mathbf{r}\,P(\mathbf{r};\mathbf{g}_1,\mathbf{g}_2)V^l(r)+\tfrac{1}{2}\sum_{i,j,\gamma,\gamma'}^{N^u,N^u}V_{aa}(|\mathbf{r}_i^\gamma-\mathbf{r}_j^{\gamma'}|)\ , \tag{2.15a}$$

or

$$W(\mathbf{Q})=\sum_\gamma\int d\mathbf{r}\,P_\gamma(\mathbf{r};\mathbf{g}_1,\mathbf{g}_2)\times\left[V^l(r)+\tfrac{1}{2}\sum_{j,\gamma'}^{N^l}V_{aa}(|\mathbf{r}-\mathbf{r}_j^{\gamma'}|)\right]\ , \tag{2.15b}$$

$$P(\mathbf{r};\mathbf{g}_1,\mathbf{g}_2)=\sum_\gamma P_\gamma(\mathbf{r};\mathbf{g}_1,\mathbf{g}_2)\ , \tag{2.16}$$

$$P_\gamma(\mathbf{r};\mathbf{g}_1,\mathbf{g}_2)=\sum_i\delta(\boldsymbol{\rho}-\Delta\boldsymbol{\rho}_i^\gamma)\delta(z-z_i^\gamma)\ , \tag{2.17}$$

where $\delta(z)$ is a δ function.

Frictional properties are studied for two cases: a rigid upper body and a relaxed upper body. In the first case, the frictional properties can be easily analyzed, and the first important result of this paper is based on this analysis. In the second, the configuration of the atoms changes either continuously or discontinuously according to displacement Q.

III. THE CASE OF AN UNRELAXED UPPER BODY

A. Adiabatic potential

It is assumed that the atoms of the upper body do not change their position coordinates due to sliding friction and that the configuration of the atoms of the upper body does not change with Q. Therefore, the first term in the right-hand side of Eq. (2.15b) is focused on, since only Q dependence of $W(\mathbf{Q})$ is of interest. The equations to be solved are

$$W(\mathbf{Q})=\sum_\gamma\int d\mathbf{r}\,P_\gamma(\mathbf{r};\mathbf{g}_1,\mathbf{g}_2)V^l(r)\ , \tag{3.1}$$

$$P_\gamma(\mathbf{r};\mathbf{g}_1,\mathbf{g}_2)=\delta(z-h_\gamma)\bar{P}_\gamma(\boldsymbol{\rho})\ , \tag{3.2}$$

$$\bar{P}_\gamma(\boldsymbol{\rho})=\sum_i\delta(\boldsymbol{\rho}-\Delta\boldsymbol{\rho}_i^\gamma)\ , \tag{3.3}$$

$$\Delta\boldsymbol{\rho}_i^\gamma=\Delta x_i^\gamma\mathbf{g}_1+\Delta y_i^\gamma\mathbf{g}_2\ , \tag{3.4}$$

where $z_i^\gamma=h_\gamma$ can designate all atoms belonging to the γth layer of the upper body, since the upper body is rigid. Equation (2.17) is then rewritten as Eq. (3.2) and h_γ is determined so as to minimize the $W(\mathbf{Q})$ for a given Q.

The frictional properties appear as the Q dependence of $\bar{P}_\gamma(\boldsymbol{\rho})$ throughout Eqs. (3.1)–(3.4). If, for example, $\bar{P}_\gamma(\boldsymbol{\rho})$ is independent on Q, a given set of h_γ is also independent on Q, since the functional form of $\mathbf{W}(\mathbf{Q})$ for h_γ does not change. Accordingly, $\bar{P}_\gamma(\boldsymbol{\rho})$ and $W(\mathbf{Q})$ are invariant for any displacement Q and the corresponding frictional force exactly vanishes. If $\bar{P}_\gamma(\boldsymbol{\rho})$ changes with Q, then $W(\mathbf{Q})$ depends on Q, and the frictional force does not vanish. Thus, the Q dependence of $\bar{P}_\gamma(\boldsymbol{\rho})$ determines the Q dependence of $W(\mathbf{Q})$, i.e., it determines whether or not the frictional force vanishes. This property is crucial in the unrelaxed case, but not so important to the relaxed case where the configuration of the atoms can discontinuously change with Q.

B. Q dependence of $\bar{P}_\gamma(\boldsymbol{\rho})$

This section examines the conditions that determine whether or not $\bar{P}_\gamma(\boldsymbol{\rho})$ is invariant for Q. To calculate

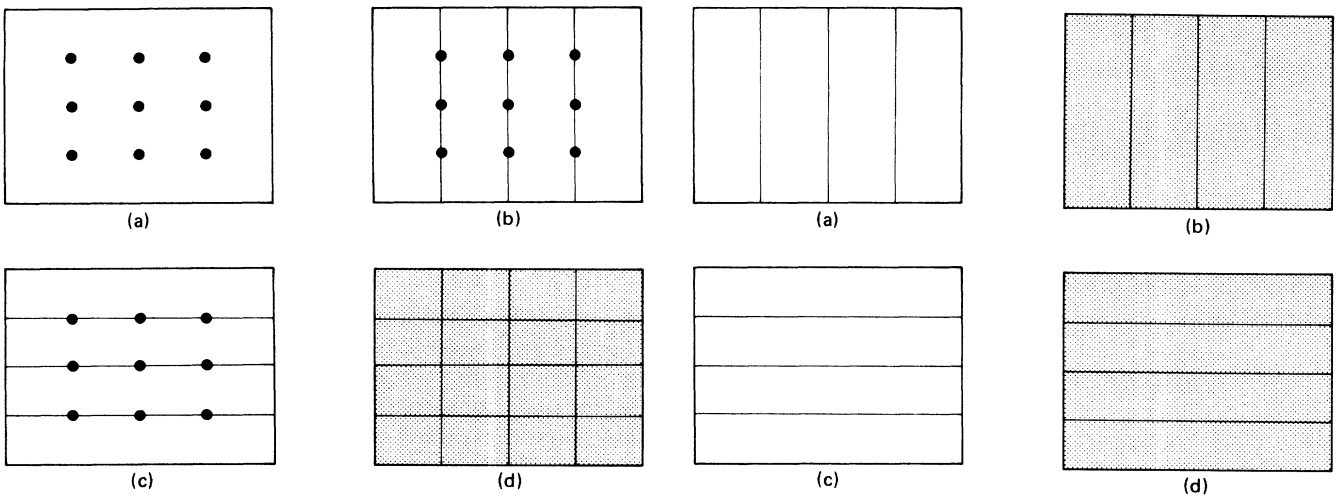

FIG. 2. Schematic illustrations of possible nonvanishing regions where the atoms of the upper body are projected onto a two-dimensional space spanned by g_1 and g_2 when $\bar{P}_\gamma(\rho)$ is variant with Q. $[(g_1',g_1)/|g_1|,\ (g_2',g_1)_i/|g_1|,\ (g_1',g_2)_i/|g_2|,\ (g_2',g_2)_i/|g_2|)]=(r,r,r,r)$ for (a), (r,r,ir,r) or (r,r,r,ir) for (b) (r,ir,r,r) or (ir,r,r,r) for (c), and $(r,\mathrm{ir},r,\mathrm{ir})$ or $(\mathrm{ir},r,r,\mathrm{ir})$ or $(r,\mathrm{ir},\mathrm{ir},r)$ or $(\mathrm{ir},r,\mathrm{ir},r)$ for (d) where r represents rationality and ir irrationality.

Δx_i^γ and Δy_i^γ in Eq. (3.4), it is necessary to specify positional vector ρ_i^γ. If the upper body is rigid, the positional vectors of the atoms belonging to the γth layer of the upper body (see Fig. 1) are

$$\rho_i^\gamma = i_1'^\gamma g_1' + i_2'^\gamma g_2' + q_0^\gamma + Q\ , \tag{3.5}$$

where q_0^γ is a misfit vector of the γth layer. Then,

$$X_i^\gamma = \frac{(\rho_i^\gamma, g_1)_i}{|g_1|} = \frac{i_1'^\gamma (g_1', g_1)_i + i_2'^\gamma (g_2', g_1)_i + (q_0^\gamma + Q, g_1)_i}{|g_1|}\ , \tag{3.6a}$$

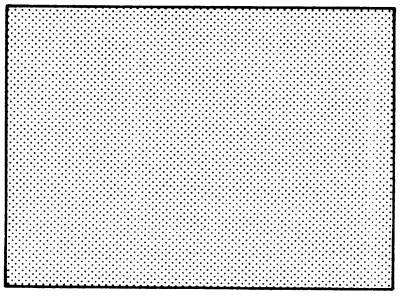

FIG. 3. Schematic illustrations of possible nonvanishing regions where the atoms of the upper body are projected onto a two-dimensional space spanned by g_1 and g_2 when $\bar{P}_\gamma(\rho)$ is invariant with Q. $[(g_1',g_1)_i/|g_1|,\ (g_2',g_1)_i/|g_1|,\ (g_1',g_2)_i/|g_2|,\ (g_2',g_2)_i/|g_2|]=(\mathrm{ir},\mathrm{ir},\mathrm{ir},\mathrm{ir})$, where ir represents irrationality.

FIG. 4. Schematic illustrations of possible nonvanishing regions where the atoms of the upper body are projected onto a two-dimensional space spanned by g_1 and g_2 when $\bar{P}_\gamma(\rho)$ invariance with Q is restricted. $[(g_1',g_1)_i/|g_1|,\ (g_2',g_1)_i/|g_1|,\ (g_1',g_2)_i/|g_2|,\ (g_2',g_2)_i/|g_2|)]=(r,r,\mathrm{ir},\mathrm{ir})$ for (a) , $(r,\mathrm{ir},\mathrm{ir},\mathrm{ir})$ or $(\mathrm{ir},r,\mathrm{ir},\mathrm{ir})$ for (b), $(\mathrm{ir},\mathrm{ir},r,r)$ for (c), and $(\mathrm{ir},\mathrm{ir},\mathrm{ir},r)$ or $(\mathrm{ir},\mathrm{ir},r,\mathrm{ir})$ for (d), where r represents rationality and ir irrationality.

$$Y_i^\gamma = \frac{(\rho_i^\gamma, g_2)_i}{|g_2|} = \frac{i_1'^\gamma (g_1', g_2)_i + i_2'^\gamma (g_2', g_2)_i + (q_0^\gamma + Q, g_2)_i}{|g_2|}\ . \tag{3.6b}$$

The two-dimensional distribution, $\bar{P}_\gamma(\rho)$, in Eq. (3.3) can be obtained according to the Bohl-Sierpinski-Weyl equipartition theorem.[8] $\bar{P}_\gamma(\rho)$ is specifically determined by projecting Δx_i^γ and Δy_i^γ onto the two-dimensional space spanned by vectors g_1 and g_2 due to Eqs. (2.13), (3.6a), and (3.6b). The equipartition theorem says that rational $(g_m',g_n)_i/|g_n|$ $(m,n=1$ or 2) results in a inhomogeneous $\bar{P}_\gamma(\rho)$, but irrational $(g_m',g_n)_i/|g_n|$ $(m,n=1$ or 2) results in a homogeneous $\bar{P}_\gamma(\rho)$. Thus, whether or not $(g_m',g_n)_i/g_n|$ $(m,n=1$ or 2) is irrational or rational determines $\bar{P}_\gamma(\rho)$. The possible combinations of $(g_m',g_n)_i/|g_n|$ generate nine kinds of $\bar{P}_\gamma(\rho)$, which are classified into three cases in terms of the Q dependence of $\bar{P}(\rho)$. The corresponding distributions of $\bar{P}(\rho)$ are schematically illustrated in Figs. 2–4.

1. Variant $\bar{P}_\gamma(\rho)$ case

Figure 2 shows $\bar{P}_\gamma(\rho)$ by lines and dots. For instance, when the values for $(g_m',g_n)_i/|g_n|$ $(m,n=1$ or 2) are all rational, $\bar{P}_\gamma(\rho)$ consists of dots seen in Fig. 2(a), since many atoms can occupy the same site in a two-dimensional space. The large dots represent a relatively high density of the projected atoms. When Q varies, the dots relocate with Q and frictional force appears. The occurrence of friction stems from the fact that the upper body moves against the lower body in the (nonflat) potential surface. This is the same as the classical picture of

friction; mechanical locking[2] of surface asperities. This potential surface, however, spans not on a large scale, but on an atomistic scale and the related mechanism is called *atomistic locking,* as an analogy for the mechanism for the mechanical locking. [This situation is later referred to as the invariant $P_1(\mathbf{r};\mathbf{g}_1,\mathbf{g}_2)$ case.]

2. *Invariant $\bar{P}_\gamma(\rho)$ case*

In Fig. 3, $\bar{P}(\rho)$ involves only the domain. The domain does not change for any direction of **Q**. As a result, the frictional force always vanishes, since $\bar{P}(\rho)$ is invariant for any **Q**. [This situation is referred to later as the invariant $P_1(\mathbf{r};\mathbf{g}_1,\mathbf{g}_2)$ case.]

3. *Restricted invariant $\bar{P}_\gamma(\rho)$ case*

In Fig. 4, $\bar{P}(\rho)$ involves lines and domains. The domains do not change for any **Q**. The lines, however, do relocate if **Q** is across the lines, but do not relocate if **Q** is along the lines. Thus, the frictional force will only vanish for **Q**, which is along the lines, but otherwise appears. [This situation is referred to later as the restricted invariant $P_1(\mathbf{r};\mathbf{g}_1,\mathbf{g}_2)$ case.]

IV. A MORE REALISTIC CASE: A RELAXED UPPER BODY

Only atoms belonging to the bottom layer of the upper body can change their position coordinates when two bodies slide against each other. This assumption is plausible, since the relaxation of atoms in the other layers, such as the 2nd, 3rd, etc. would probably be small compared to those of the bottom layer. Two extreme limits for $V^l(r)$ (weak and strong) are studied to see what occurs when $V_{ab}(r)$ becomes stronger.

A. Weak limit

The three-dimensional distribution, $P_1(\mathbf{r};\mathbf{g}_1,\mathbf{g}_2)$, in Eq. (2.17) is studied instead of $\bar{P}_\gamma(\rho)$ in Eq. (3.3). The adiabatic potential consists of the following three interactions: $V^l(r)$, $V^u(r)$, and U, which the atoms in the bottom layer receive. $V^l(r)$ is the interaction from the atoms of the lower body. $V^u(r)$ is the interaction from the atoms of the 2nd, 3rd, etc., layers of the upper body. U is the mutual interaction that occurs between atoms belonging to the bottom layer of the upper body:

$$W(\mathbf{Q})=\sum_i V^l(r_i^1)+\sum_i V^u(r_i^1)+U \ , \tag{4.1}$$

where

$$V^l(r)=\sum_j^{N^l} V_{ab}(|\mathbf{r}-\mathbf{r}_j|) \ , \tag{4.2}$$

$$V^u(r)=\sum_{j,\gamma\neq 1} V_{aa}(|\mathbf{r}-\mathbf{r}_j^\gamma|) \ , \tag{4.3}$$

$$U=\tfrac{1}{2}\sum_{i,j} V_{aa}(|\mathbf{r}_i^1-\mathbf{r}_j^1|) \ . \tag{4.4}$$

Since $V_{ab}(r)$, i.e., $V^l(r)$ is weak $r_i^{1,\alpha}$ ($\alpha=x$, y, or z) is expected to be very close to the position coordinate obtained by assuming a rigid upper body. Putting $r_i^{1,\alpha}=r_{i,0}^{1,\alpha}+\Delta r_i^\alpha$ (or $\mathbf{r}_i^1=\mathbf{r}_{i,0}^1+\Delta\mathbf{r}_i$) into Eqs. (4.2)–(4.4), and then expanding by a small Δr_i^α (or $\Delta\mathbf{r}_i$), we have

$$\sum_i V^l(r_i)=\sum_i V^l(r_{i,0})+\sum_{i,\alpha}\frac{\partial V^l(r_{i,0}^l)}{\partial r_{i,0}^{1,\alpha}}\Delta r_i^\alpha + \tfrac{1}{2}\sum_{i,\alpha,\beta} V_{i,i}^{l,\alpha,\beta}\Delta r_i^\alpha\Delta r_i^\beta \ , \tag{4.5}$$

$$\sum_i V^u(r_i)=\sum_i V^u(r_{i,0})+\sum_{i,\alpha}\frac{\partial V^u(r_{i,0}^l)}{\partial r_{i,0}^{1,\alpha}}\Delta r_i^\alpha + \tfrac{1}{2}\sum_{i,\alpha,\beta} V_{i,i}^{u,\alpha,\beta}\Delta r_i^\alpha\Delta r_i^\beta \ , \tag{4.6}$$

$$U=\sum_{i,j} V_{aa}(|\mathbf{r}_{i,0}^1-\mathbf{r}_{j,0}^1|)+\tfrac{1}{2}\sum_{i,j,\alpha,\beta} U_{i,j}^{\alpha,\beta}\Delta r_i^\alpha\Delta r_j^\beta \ , \tag{4.7}$$

where

$$V_{i,i}^{l,\alpha,\beta}=\frac{\partial^2 V^l(r_{i,0})}{\partial r_{i,0}^{1,\alpha}\partial r_{i,0}^{1,\beta}} \ , \tag{4.8}$$

$$V_{i,i}^{u,\alpha,\beta}=\frac{\partial^2 V^u(r_{i,0})}{\partial r_{i,0}^{1,\alpha}\partial r_{i,0}^{1,\beta}} \ , \tag{4.9}$$

$$U_{i,j}^{\alpha,\beta}=\frac{\partial^2 V_{aa}(r_{ij,0}^1)}{\partial r_{ij,0}^{1,\alpha}\partial r_{ij,0}^{1,\beta}} \quad \text{for } i\neq j \ , \tag{4.10a}$$

$$U_{i,i}^{\alpha,\beta}=-\sum_j\frac{\partial^2 V_{aa}(r_{ij,0}^1)}{\partial r_{ij,0}^{1,\alpha}\partial r_{ij,0}^{1,\beta}} \quad \text{for } i=j \ , \tag{4.10b}$$

where $r_{ij,0}^{1,\alpha}=r_{i,0}^{1,\alpha}-r_{j,0}^{1,\alpha}$. $U_{i,j}^{\alpha,\beta}$ satisfies the relationship $U_{i,i}^{\alpha,\beta}+\sum_{j(\neq 1)}U_{i,j}^{\alpha,\beta}=0$ for $\alpha,\beta=x$, y, or z. This is equivalent to a condition where interaction U has translational invariance, that is, U is invariant for the uniform displacements $\mathbf{r}_i\rightarrow\mathbf{r}_i+\mathbf{a}$ (**a** denotes arbitrary constant displacement vector) of all the atoms.

When one chooses $r_{i,0}$ so as to minimize $\sum_i V^u(r_i)+U$, the adiabatic potential can be obtained by minimizing

$$W(\mathbf{Q}:\{\Delta r_i^\alpha\})=\sum_i V^l(r_{i,0}^1)+\sum_i V^u(r_{i,0}^1)+\sum_{i,j} V_{aa}(|\mathbf{r}_{i,0}^1-\mathbf{r}_{j,0}^1|)+\sum_{i,\alpha}\frac{\partial V^l(r_{i,0}^1)}{\partial r_{i,0}^{1,\alpha}}\Delta r_i^\alpha+\tfrac{1}{2}\sum_{i,\alpha,\beta}[\epsilon_{i,j}(V_{i,j}^{l,\alpha,\beta}+V_{i,j}^{u,\alpha,\beta})+U_{i,j}^{\alpha,\beta}]\Delta r_i^\alpha\Delta r_j^\beta \tag{4.11}$$

with respect to Δr_i^α, where $\epsilon_{ij}=1$ for $i=j$ and $\epsilon_{i,j}=0$ otherwise. The atoms in the bottom layer feel a stronger potential from the atoms in the upper layers (2nd, 3rd, etc.) than from those in the same bottom layer for a first approximation. The interaction from the bottom layer is actually $\frac{1}{10}$ to $\frac{1}{2}$ that from the upper layers of the fcc and bcc lattices. The mutual interaction term $U_{i,j}^{\alpha,\beta}$ is neglected for the first approximation. The derivation of the po-

sition coordinates for the atoms of the upper body can be obtained from the Appendix by taking $U_{i,j}^{\alpha,\beta}$ into account. Then it is set that $V_{i,i}^{u_i x,x}=\omega_x>0$, $V_{i,i}^{u_i y,y}=\omega_y>0$, $V_{i,i}^{u_i z,z}=\omega_z>0$, and $U_{i,j}^{\alpha,\beta}=0$ in Eq. (4.11) for surfaces such as the (001) planes of the bcc lattices which have a square symmetry. For other cyrstal planes, the results are slightly modified. Displacement Δr_i^α, as obtained from Eq. (4.11), is

$$\Delta r_i^\alpha \simeq -\frac{\partial V^l(r_{i,0})/\partial r_{i,0}^\alpha}{V_{i,i}^{u_i\alpha,\alpha}} = -\frac{\partial V^l(r_{i,0})/\partial r_{i,0}^\alpha}{\omega_\alpha} \ . \quad (4.12)$$

This expression tells us that Δr_i^α continuously changes if $\partial V^l(r_i^\alpha)/\partial r_i^\alpha$ is a continuous function of r_i^α. In the case of a rigid upper body, $P_1(\mathbf{r};\mathbf{g}_1,\mathbf{g}_2)$ is obtained as $P_1(\mathbf{r};\mathbf{g}_1,\mathbf{g}_2)=\delta(z-h_1)\sum_i\delta(\boldsymbol{\rho}-\Delta\boldsymbol{\rho}_i^1)=\delta(z-h_1)\bar{P}_1(\boldsymbol{\rho})$. $P_1(\mathbf{r};\mathbf{g}_1,\mathbf{g}_2)$ consists of nonvanishing regions that involve the lines, dots, or domains shown in Figs. 2–4. For the weak $V^l(r)$, each point in the regions slightly shifts in accordance with Eq. (4.12), even though the lines, dots, or domains do not change their topology when shifts occur due to a weak $V^l(r)$. Thus, the frictional properties for a weak $V^l(r)$ are essentially the same as those in the rigid upper-body case, provided the first derivative of $V^l(r)$ is a continuous function of r.

As seen in Eq. (4.12), the density of $P_1(\mathbf{r};\mathbf{g}_1,\mathbf{g}_2)$ generally decreases as one approaches the ridge lines of $V^l(r)$. The direction along the ridge line is defined as $\partial V^l(r)/\partial r=0$ and $\partial^2 V^l(r)/\partial r^2<0$ as the direction perpendicular to it. These ridge lines play a crucial role in deciding whether or not the frictional force vanishes and they will be discussed later.

B. Strong limit

Atoms in the bottom layer of the upper body position themselves at the lowest minima of potential $V^l(r)$ that is the nearest to each atom. These lowest minima positions are denoted by vectors $i_1\mathbf{g}_1+i_2\mathbf{g}_2+\tau_m$ (i_1,i_2=any integer), where m denotes only one minimum when there are several lowest minima in the primitive cell of the lower body. For the (001) planes of simple crystals, such as bcc lattices $m=1$. Integers i_1 and i_2 in $\mathbf{i}_1\mathbf{g}_1+i_2\mathbf{g}_2+\tau_m$ nearest to $\boldsymbol{\rho}_i=i_1'\mathbf{g}_1'+i_2'\mathbf{g}_2'+\mathbf{q}_0+\mathbf{Q}$ are determined so as to minimize the distance

$$d_{i_1,i_2}=|(\mathbf{i}_1\mathbf{g}_1+i_2\mathbf{g}_2+\tau_m)-(\boldsymbol{\rho}_i=i_1'\mathbf{g}_1'+i_2'\mathbf{g}_2'+\mathbf{q}_0+\mathbf{Q})|$$

for a certain m . (4.13)

$P_1(\mathbf{r};\mathbf{g}_1,\mathbf{g}_2)$ is invariant for any $\mathbf{Q}$, since the atoms definitely occupy the positions of the lowest minima of $V^l(r)$.

Let us consider the frictional system shown in Fig. 5. A small displacement of $\mathbf{Q}$ changes a few i_1 (or i_2) into $i_1\pm1$ (or $i_2\pm1$). A few corresponding atoms then jump from site $i_1\mathbf{g}_1+i_2\mathbf{g}_2+\tau_m$ to the nearest-neighboring site. Frictional energy is necessary for the atoms to change beyond the potential barrier between site $i_1\mathbf{g}_1+i_2\mathbf{g}_2+\tau_m$ and its nearest-neighboring site. Frictional force then appears, identifying another origin of friction. The atoms

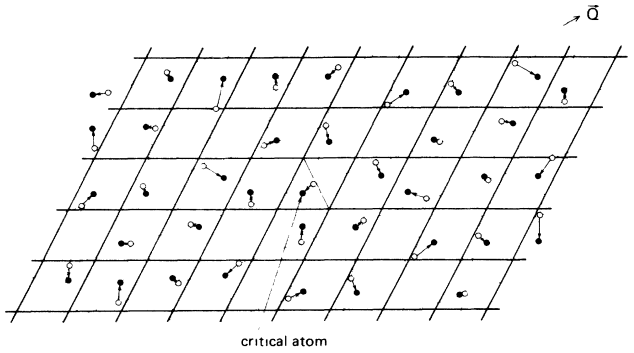

FIG. 5. Two contacting surfaces where $P_1(\mathbf{r};\mathbf{g}_1,\mathbf{g}_2)$ of the frictional system is invariant for any $\mathbf{Q}$. The upper-body surface, shown by dashed lines, contacts the lower-body surface, shown by solid lines. Atoms initially positioned at symbols (○) move symbols (●), which correspond to the lowest minimum of $V^l(r)$. The critical atom near the boundary line of a primitive cell of the lower body is the one most likely to jump beyond the potential barrier when $\mathbf{Q}$ is given.

discontinuously change. The appearance of the discontinuity is ascribed to the failure of the adiabatic potential description. This origin, therefore, cannot be described within the framework of the adiabatic potential. The origin can be described only by taking the dynamic movements of the atoms into account. Accordingly, this origin of frictional forces is referred to as *dynamic locking*. $P_1(\mathbf{r};\mathbf{g}_1,\mathbf{g}_2)$ is still invariant in this displacement. Dynamic locking occurs for any arbitrarily small displacement $\mathbf{Q}$. Frictional force is, therefore, a complicated function of $\mathbf{Q}$.

In the invariant $P_1(\mathbf{r};\mathbf{g}_1,\mathbf{g}_2)$ case, dynamic locking occurs infrequently. When a certain $\mathbf{Q}$ is given, many of the atoms throughout the entire system cooperatively jump beyond the potential barrier, since $(\mathbf{g}_m',\mathbf{g}_n)_i/|\mathbf{g}_n|$ ($m,n=1$ or 2) is rational. In the restricted invariant $P_1(\mathbf{r};\mathbf{g}_1,\mathbf{g}_2)$ case, dynamic locking frequently occurs only in a direction along the lines in $P_1(\mathbf{r};\mathbf{g}_1,\mathbf{g}_2)$.

C. Intermediate regime: Friction transition

In the variant $P_1(\mathbf{r};\mathbf{g}_1,\mathbf{g}_2)$ case, the nonvanishing regions of $P_1(\mathbf{r};,\mathbf{g}_1,\mathbf{g}_2)$ consist of many dots or lines (see Fig. 2) for an arbitrary strength of $V^l(r)$. $P_1(\mathbf{r};\mathbf{g}_1,\mathbf{g}_2)$ varies for any $\mathbf{Q}$ and any $V^l(r)$. When $\mathbf{Q}$ varies, the atoms in the upper body continuously change their positions. This leads to atomistic locking, resulting in nonvanishing frictional force. The corresponding adiabatic potential and frictional force is calculated by specifying the functional form of interaction $V_{ab}(r)$. As $V^l(r)$ becomes stronger, the vanishing region (where atoms cannot stay) broadens in $P_1(\mathbf{r};\mathbf{g}_1,\mathbf{g}_2)$ for any $\mathbf{Q}$. Further increases in $V^l(r)$ disconnect the pattern where $P_1(\mathbf{r};\mathbf{g}_1,\mathbf{g}_2)$ is tiled periodically, as shown in Fig. 6(a), depending on the direction of $\mathbf{Q}$. When $\mathbf{Q}$ in the disconnected direction is given, the atoms only move by nonadiabatic jumping over the vanishing regions in $P_1(\mathbf{r};\mathbf{g}_1,\mathbf{g}_2)$. This leads to

dynamic locking.

In the invariant $P_1(\mathbf{r};\mathbf{g}_1,\mathbf{g}_2)$ case, the nonvanishing region in $P_1(\mathbf{r};\mathbf{g}_1,\mathbf{g}_2)$ consists of only the domain (see Fig. 3) for a weak $V^l(r)$. $P_1(\mathbf{r};\mathbf{g}_1,\mathbf{g}_2)$ is invariant for any Q and for a small $V^l(r)$, resulting in vanishing frictional force. Atomistic locking never occurs under these circumstances. As $V^l(r)$ becomes stronger, the vanishing region appears in $P_1(\mathbf{r};\mathbf{g}_1,\mathbf{g}_2)$. Further increases in $V^l(r)$ eventually disconnect the pattern where $P_1(\mathbf{r};\mathbf{g}_1,\mathbf{g}_2)$ is periodically tiled, shown in Fig. 6(b), depending on the direction of Q. This results in dynamic locking due to a strong $V^l(r)$ interaction. It can thus be concluded that the transition where frictional force changes from vanishing to finite occurs due to an increased $V^l(r)$. This transition is called *friction transition.*

In the restricted invariant $P_1(\mathbf{r};\mathbf{g}_1,\mathbf{g}_2)$ case, the nonvanishing regions consist of lines and dots (see Fig. 4) if $V^l(r)$ is weak. $P_1(\mathbf{r};\mathbf{g}_1,\mathbf{g}_2)$ is invariant for a Q along the lines in $P_1(\mathbf{r};\mathbf{g}_1,\mathbf{g}_2)$ and for a weak $V^l(r)$, which results in the occurrence of vanishing frictional force only along those lines. Increases in $V^l(r)$ will cause the pattern for $P_1(\mathbf{r};\mathbf{g}_1,\mathbf{g}_2)$ to disconnect, depending on the direction of Q. After this disconnectedness, dynamic locking occurs.

There are two atomistic origins for solid sliding friction; atomistic locking and dynamic locking. One locking concept stems from the fact that all the atoms of a contact surface will cooperatively move as seen in the variant and the restricted invariant $P_1(\mathbf{r};\mathbf{g}_1,\mathbf{g}_2)$ cases. The other stems from the fact that atoms independently jump beyond the nearest-neighboring potential barrier due to nonadiabatic effects, as seen in all cases with a strong $V^l(r)$. It was then found that both the Q dependence of $P_1(\mathbf{r};\mathbf{g}_1,\mathbf{g}_2)$ and the changes in the topological properties of the patterns made by $P_1(\mathbf{r};\mathbf{g}_1,\mathbf{g}_2)$ determine

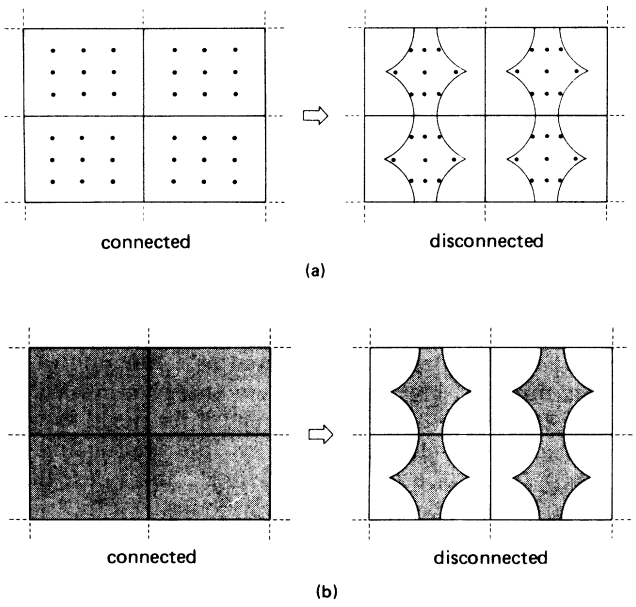

FIG. 6. Disconnectedness of a pattern made by tiling $P_1(\mathbf{r};\mathbf{g}_1,\mathbf{g}_2)$ periodically. (a) is the variant $P_1(\mathbf{r};\mathbf{g}_1,\mathbf{g}_2)$ case, and (b) is the invariant $P_1(\mathbf{r};\mathbf{g}_1,\mathbf{g}_2)$ case.

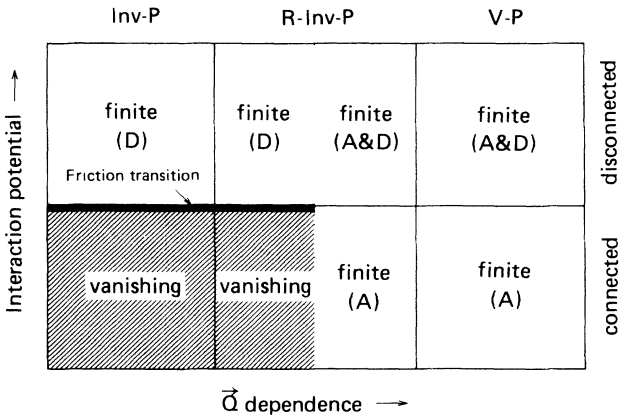

FIG. 7. Schematic phase diagram representing whether or not frictional force is finite or vanishing. Here, the invariant $P_1(\mathbf{r};\mathbf{g}_1,\mathbf{g}_2)$ case is denoted as Inv-*P*, the restricted invariant $P_1(\mathbf{r};\mathbf{g}_1,\mathbf{g}_2)$ case as *R*-Inv-*P*, and the variant $P_1(\mathbf{r}_1;\mathbf{g}_1,\mathbf{g}_2)$ case as *V*-*P*. Atomistic locking is denoted as (*A*), and dynamic locking as (*D*).

the frictional properties in both the unrelaxed and relaxed upper-body cases. A summarized diagram of this is shown in Fig. 7 and forms the central results of this paper.

Friction transition is the same as the transition of analyticity breaking, often called Aubry transition.[9] Aubry studied the Frenkel-Kontrowa model which is a one-dimensional system to describe the movement of defects or dislocations. Analyticity breaking corresponds to the discontinuous change of the relaxed particle positions. For restricted invariant and invariant $P_1(\mathbf{r};\mathbf{g}_1,\mathbf{g}_2)$ the relaxed particle positions discontinuously change as Q varies. The friction transition demonstrates the Aubry transition for the two-dimensional system.

D. Friction transition: Criterion for its occurrence

A condition needs to be derived to decide whether or not friction transition occurs. Three interactions are considered for this condition: $V^l(r)$, $V^u(r)$, and $U=(\frac{1}{2})\sum_{i,j}V_{aa}(|\mathbf{r}_i^1-\mathbf{r}_j^1|)$. The first two can be regarded as the external local fields that act on each atom belonging to the bottom layer of the upper body. The last is the mutual interaction term for the atoms belonging to the bottom layer of the upper body. The (approximated) criterion is obtained for a case where interaction $V^l(r)$ is sufficiently strong (cf. discussion in Sec. IV A) and the derived criterion for a general case is shown in the Appendix.

A simple case involving a one-dimensional system is first studied, in which only $V^l(r)$ and $V^u(r)$ operate (see Fig. 8). The results of that case are extended to our two-dimensional system. When $V^l(r)=0$, the atoms occupy positions that correspond to the lowest minima of $V^u(r)$. For a weak $V^l(r)$ limit, the atoms change their positions slightly towards the minimum positions of $V^l(r)$. For a strong $V^l(r)$ limit, the atoms occupy positions that correspond to the lowest minima of $V^l(r)$. When distribution

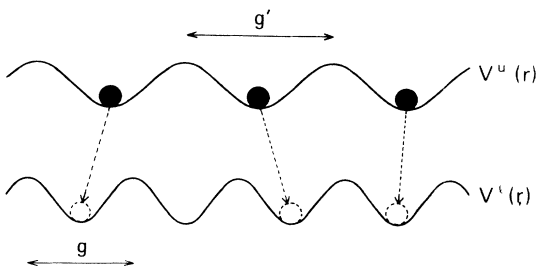

FIG. 8. A one-dimensional frictional system. $V^l(r)$ and $V^u(r)$ have their periodicities characterized by lengths g and g'. The atoms sit on the lowest minima (●) of $V^u(r)$, when $V^l(r)=0$. When $V^l(r)$ becomes a strong limit, the atoms occupy the positions for the lowest minima (○) of $V^l(r)$.

$\bar{P}(r)$ is periodically arranged in a one-dimensional space, the nonvanishing regions in $\bar{P}(r)$ connect with each other for a weak $V^l(r)$, but disconnect for a strong $V^l(r)$. The friction transition that then occurs is similar to the two-dimensional case just previously mentioned and a criterion for it can be derived.

The potential energy is $V^l(r)+V^u(r)$, when r is close to the position of the extreme maxima of $V^l(r)$ and to that of the lowest minima of $V^u(r)$. If $r=r_{\max}+\Delta r$ and $r=r_{\min}+\Delta r'$, and $V^l(r)+V^u(r)$ is expanded by a small Δr and $\Delta r'$, then

$$V^l(r)+V^u(r)=V^l(r_{\max})+V^u(r_{\min})+\Delta r^2[d^2V^l(r_{\max})/dr_{\max}^2]+\Delta r'^2[d^2V^u(r_{\min})/dr_{\min}^2] .$$

Atoms are unable to occupy vanishing regions in $\bar{P}(r)$. The potential is concave function at these positions. Since Δr is a function of $\Delta r'$, $\Delta r=r_{\min}-r_{\max}+\Delta r'$, and the condition under which Δr or $\Delta r'$ becomes unstable is

$$\frac{d^2V^l(r_{\max})}{dr_{\max}^2}+\frac{d^2V^u(r_{\min})}{dr_{\min}^2}<0 . \tag{4.14}$$

When $d^2V^l(r_{\max})/dr_{\max}^2+d^2V^u(r_{\min})/dr_{\min}^2 \geq$ (or $<$) 0, frictional force vanishes (or appears).

Let us extend this criterion to a two-dimensional system. First, consider the case where $U=0$. $r_{\max}$ of $V^l(r)$ corresponds to a point satisfying $\partial V^l(r)/\partial r=0$ and $\partial^2V^l(r)/\partial r^2<0$ along lines that are perpendicular to the ridge lines of $V^l(r)$. For basal planes such as the (001) planes of bcc lattices, the ridge lines are obtained by connecting four points of a square spanned by the two primitive vectors $\mathbf{g}_1$ and $\mathbf{g}_2$. The position on the ride lines is denoted as $\mathbf{r}_s$ [or (r_s^x,r_s^y)]. $r_{\min}$ of $V^u(r)$ corresponds to the lowest minima of $V^u(r)$. The potential energy expanded by a small Δr^x and Δr^y, and $\Delta r'^x$ and $\Delta r'^y$ are

$$V^l(r_s)+V^u(r_{\min})+\sum_{\alpha,\beta}V^l_{\alpha,\beta}(r_s)\Delta r^\alpha\Delta r^\beta+\sum_{\alpha,\beta}V^u_{\alpha,\beta}(r_{\min})\Delta r'^\alpha\Delta r'^\beta . \tag{4.15}$$

If the relationship between $(\Delta r^x,\Delta r^y)$ and $(\Delta r'^x,\Delta r'^y)$ is given as

$$\Delta r'^\alpha=\sum_\gamma T_{\alpha,\gamma}\Delta r^\gamma , \tag{4.16}$$

then Eq. (4.15) becomes

$$V^l(r_s)+V^u(r_{\min})+\sum_{\alpha,\beta}\left[V^l_{\alpha,\beta}(r_s)+\sum_{\gamma,\gamma'}(r_{\min})T_{\gamma,\alpha}T_{\gamma',\beta}\right]\Delta r^\alpha\Delta r^\beta . \tag{4.17}$$

The condition that the potential energy is a concave function of r for a one-dimensional system is equivalent to the condition that the potential energy is a concave function in a direction that is perpendicular to the ridge lines for a two-dimensional system. Denoting this direction perpendicular to the ridge lines as vector $\mathbf{s}=(s_x,s_y)$, the corresponding condition is

$$V_{x,x}s_x^2+2V_{x,y}s_xs_y+V_{y,y}s_y^2<0 , \tag{4.18}$$

where $V_{\alpha,\beta}$ is defined by

$$V_{\alpha,\beta}=V^l_{\alpha,\beta}(r_s)+\sum_{\gamma,\gamma'}V^u_{\gamma,\gamma'}(r_{\min})T_{\gamma,\alpha}T_{\gamma',\beta}+\sum_m U_{\alpha,\beta}(|\mathbf{s}-\mathbf{r}^{l,m}|) . \tag{4.19}$$

The effects introduced by mutual interaction U are taken in account by adding the last term in the right-hand side of Eq. (4.19)

V. FRICTIONAL PROPERTIES FOR VARIOUS SYSTEMS

A. Quasistatic friction of α-iron

In this section, realistic calculations are demonstrated that relate to the quasistatic sliding friction of α-iron. The adiabatic potentials, calculated as a function of the sliding distance, give the minimum energy necessary for sliding friction to occur. Two types of frictional systems are examined, characterized by the rationality of $(\mathbf{g}'_m,\mathbf{g}_n)_i/|\mathbf{g}_n|$ $(m,n=1$ or 2), where $\mathbf{g}'_m$ and $\mathbf{g}_n$ are primitive vectors of the upper and lower bodies.

Case (a). The (001) plane of α-iron (bcc lattice) is placed against another (001) plane, as shown in Fig. 9(a). The upper body is then slid against the lower one in direction x. The bcc lattices that have a unit vector of $\mathbf{T}=(a,a,a)$ (a denotes a lattice constant of the bcc lattice) for the upper body are placed on the same bcc lattices of the lower body. This contact generates the variant

$P_1(\mathbf{r};\mathbf{g}_1,\mathbf{g}_2)$ case [see Fig. 2(a)]: since both $(\mathbf{g}_1,\mathbf{g}_1)_i/|\mathbf{g}|$ and $(\mathbf{g}_2',\mathbf{g}_2)_i/|g_2|$ are rational, $(\mathbf{g}_2',\mathbf{g}_1)_i/|\mathbf{g}_1|=0$, and $(\mathbf{g}_1',\mathbf{g}_2)_i/|\mathbf{g}_2|=0$. The upper-body lattice is then commensurate with the lower-body lattice both in its sliding direction x and vertical direction y.

Case (b). The (110) plane of α-iron is placed against a (001) plane, as shown in Fig. 9(b). The upper body is slid against the lower one in direction x. The fct (face-centered tetragonal) lattices that have a unit vector of $\mathbf{T}=(a,\sqrt{2}a,a)$ for the upper body are placed on the bcc lattices that have a unit vector of $\mathbf{T}=(a,a,a)$ for the lower body. This contact generates the restricted invariant $P_1(\mathbf{r};\mathbf{g}_1,\mathbf{g}_2)$ case [see Fig. 4(c)]: since $(\mathbf{g}_1',\mathbf{g}_1)_i/|\mathbf{g}_1|$ and $(\mathbf{g}_1',\mathbf{g}_2)_i/|\mathbf{g}_2|$ are rational, $(\mathbf{g}_2',\mathbf{g}_2)_i/|\mathbf{g}_2|$ is irrational, and $(\mathbf{g}_2',\mathbf{g}_1)_i/|\mathbf{g}_1|=0$. The upper-body lattice is then commensurate with the lower-body lattice in sliding direction x, while being incommensurate in vertical direction y.

Several kinds of interatomic potentials[10–13] have been proposed for α-iron. The Johnson potential was chosen from among them since it has been successfully used to calculate such atomic displacements as the tensile deformations of amorphous iron.[14] This potential is expressed as three third-order polynomials:

$$\phi(r)=-2.195\,976(r-3.097\,910)^3+2.704\,060r-7.436\,448\ \text{eV}\quad \text{for } 1.9\ \text{Å}<r\le 2.4\ \text{Å}, \tag{5.1a}$$

$$\phi(r)=-0.639\,230(r-3.115\,829)^3+0.477\,871r-1.581\,570\ \text{eV}\quad \text{for } 2.4\ \text{Å}<r\le 3.0\ \text{Å}, \tag{5.1b}$$

$$\phi(r)=-1.115\,035(r-3.066\,403)^3+0.466\,892r-1.547\,967\ \text{eV}\quad \text{for } 3.0\ \text{Å}<r\le 3.44\ \text{Å}. \tag{5.1c}$$

The α-iron lattice constant is taken as 2.86 Å. The model potential can yield reasonable surface energies for α-iron:

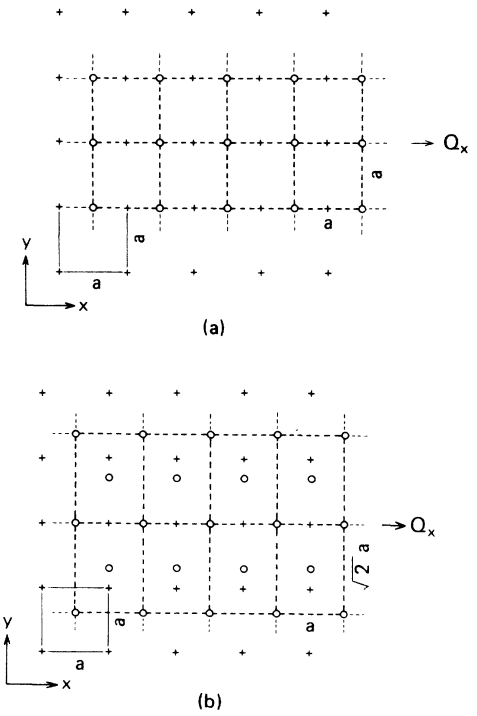

FIG. 9. Atomic arrangements at the contact interfaces. The upper body with atoms (○) is slid over a stationary lower body with atoms (+) in the x direction. $P_1(\mathbf{r};\mathbf{g}_1,\mathbf{g}_2)$ is variant with $\mathbf{Q}$ in any direction for (a). $P_1(\mathbf{r};\mathbf{g}_1,\mathbf{g}_2)$ is still variant with any $\mathbf{Q}$ for (b).

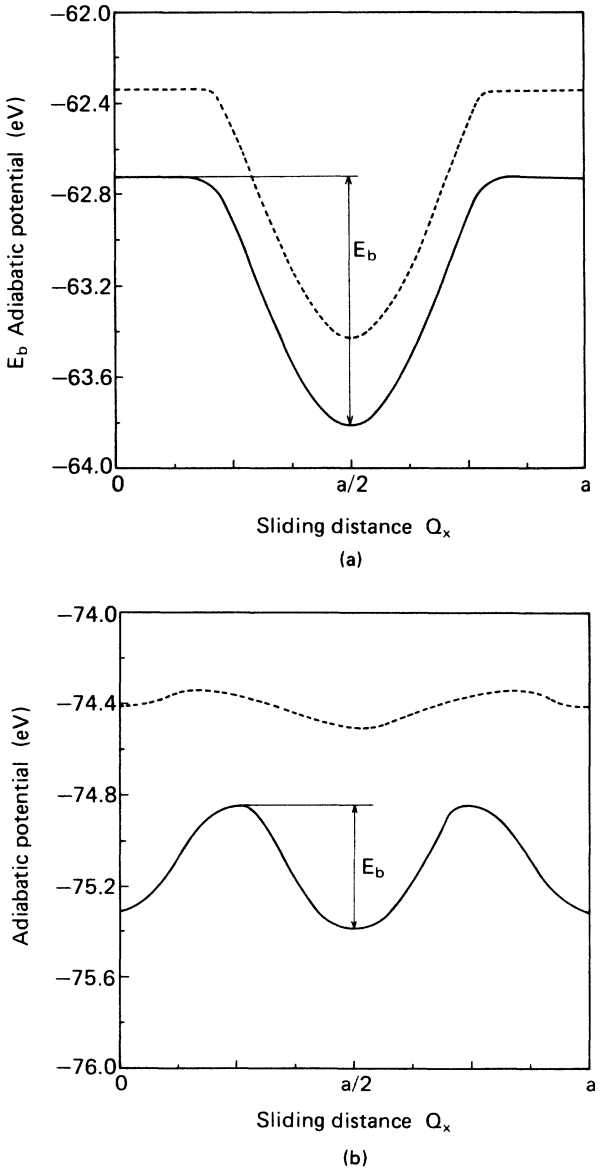

FIG. 10. Calculated adiabatic potentials normalized by the contact area. The (001) plane of α-iron is slid over the same (001) plane for (a), and a (110) plane over a (001) plane for (b). Dashed lines represent the unrelaxed case and solid lines the relaxed one.

1.31 J/m^2 for the (001) plane and 1.21 J/m^2 for the (110) plane. These values are comparable to a measured surface energy of 2.2 J/m^2.[15] The frictional properties of the rigid upper-body case are compared with those of the relaxed upper-body case. To do this comparison, the system used is assumed to be of a sufficiently large, but finite size. The size of the adopted system is (20×20×2) bcc unit cells (2123 atoms) for the upper body and (24×24×2) bcc unit cells (3027 atoms) for the lower body in case (a), and (20×20×2) fct unit cells (4203 atoms) for the upper body and (24×32×2) bcc unit cells (4011 atoms) for the lower body in case (b).

Figure 10 shows adiabatic potentials normalized by contact area A as a function of sliding distance Q_x in cases (a) and (b). Potential barrier E_b can be observed in both cases. E_b changes only slightly after relaxation in case (a), but it increases noticeably after relaxation in case (b). Potential barrier E_b in case (b) is smaller than that in case (a), so less frictional force appears in case (b). Calculation shows that $E_b=1.1$ J/m^2 in case (a), and $E_b=0.53$ J/m^2 in case (b). The average frictional forces calculated by Eq. (2.6) are $F_{av}(\mathbf{Q}_1,\mathbf{Q}_2)=7.6$ GPa in case (a), and $F_{av}(\mathbf{Q}_1,\mathbf{Q}_2)=3.7$ GPa in case (b). Unfortunately, directly comparable experimental data are not available. Current experiments[5,6] have shown highly resolved frictional force distributions with a sensitivity ranging from 1×10^{-7} to 1×10^{-6} N by scanning very sharp 0.1 to 5 μm radius tips of diamond or tungsten over a sputtered carbon film or a highly oriented polycrystalline graphite. The frictional forces measured are normalized by the apparent elastically contacting area and range from about 0.1 GPa to a few GPa. This suggests that the frictional force resulting from atomistic locking is comparable to the frictional force that will be measured in future experiments.

Another finding is that the amount of adhesion force has no relation to the frictional force amount. Frictional force has often been ascribed to adhesion, i.e., chemical bonding between the actual contact surfaces in phenomenological studies.[4] In those studies, adhesion occurs at the actual contact area where the external load is concentrated. This concentrated load moves surface contaminants from the contact area, thus possibly causing the formation of adhered junctions. Accordingly, shearing force has to be applied to rupture the adhered junctions during subsequent sliding friction. Frictional force can, therefore, depend on shear strength and on the actual contact area where the adhered junctions are formed. When plastic deformations are introduced into the adhered junctions, the junction growth can actually be observed.[16] Our results, however, did not show a relationship between adhesion force and frictional force.

B. Validity of the criterion for friction transition

The criterion for friction transition states that friction transition occurs when second-order derivative $V_{\alpha,\beta}$, in a direction perpendicular to a $V^l(r)$ ridge line, is negative. If distribution $P_1(\mathbf{r};\mathbf{g}_1,\mathbf{g}_2)$ is considered just before the friction transition occurs, the pattern is still connected by one atom (this atom is hereafter called the critical atom) on the ridge line. The occurrence of friction transition can, therefore, be decided by judging whether or not $V_{\alpha,\beta}$ in Eq. (4.19) is negative at the critical atom position.

The model verifies this consists of two contacting bodies, the (001) plane of α-iron (upper body) that faces against the (110) plane of α-iron (lower body) at a 30° angle as shown in Fig. 11. The upper body is placed against the lower body so that the critical atom is positioned at the midpoint on the boundary line of the two-dimensional primitive cell of the lower body, where the critical atom feels the local minimum of the potential from the upper body, $V^u(r_{min})$, and the local maximum from the lower body, $V^l(r_{max})$. The upper body is taken to have (20×20×2) bcc unit cells (4203 atoms) with a unit vector of $\mathbf{T}=(a,a,a)$ and the lower body (24×32×2) fct unit cells (4011 atoms) with a unit vector of $\mathbf{T}=(\sqrt{2}a,a,\sqrt{2}a)$. At the beginning of the calculation, the rigid upper body is placed so as to minimize the total crystal energy by adjusting the interfacial separation. Next, the atoms in the upper body, excluding the critical atom, are relaxed three dimensionally, while all of the atoms in the lower body are fixed. Two kinds of potentials are used, the Morse potential and the Johnson potential, as the interatomic potentials operating in the system. The Morse potential expressed as $V(r)=D(e^{-2\alpha(r-r_0)}-2e^{-\alpha(r-r_0)})D,\alpha,r_0$: potential parameter), and is selectively applied to the atoms on the contact interface. The Johnson potential is used for the other atoms.

As seen in Sec. IV D, the critical atom is assumed to sit on the local minimum of $V^u(r_{min})$. This assumption was confirmed by actual calculation. The calculated second-order derivatives of potential $V_{\alpha,\beta}$ in Eq. (4.19) are shown as a function of Morse potential parameter D in Fig. 12. $V_{\alpha,\beta}$ decreases as D increases, since negative contribution $V^l(r_{max})$ from the lower body increases. The friction

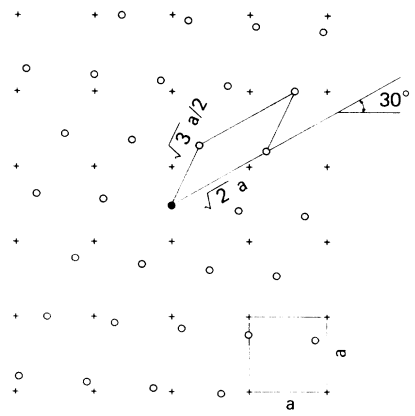

FIG. 11. Model for friction transition. (○) symbols are upper-body atoms, and (+) symbols are lower-body atoms. The (●) symbol is the critical atom.

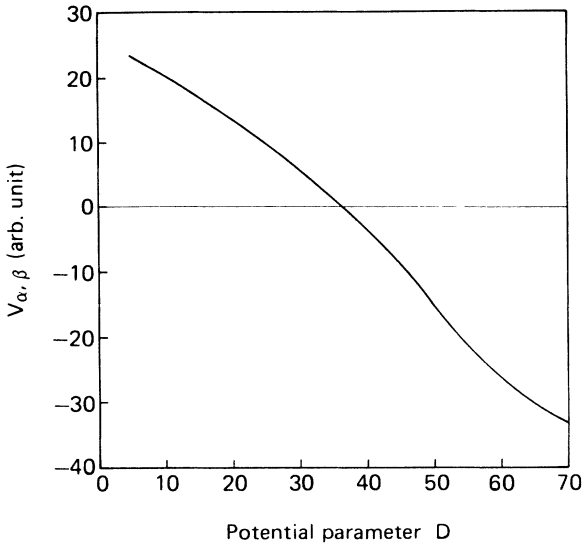

FIG. 12. Calculated $V_{\alpha,\beta}$ as a function of Morse potential parameter D.

transition actually occurs when D is approximately 35. Figure 13 shows distribution $P_1(\mathbf{r};\mathbf{g}_1,\mathbf{g}_2)$ before relaxation and after relaxation when $D=10$, 20, and 60. The atoms initially move from the region around the corner of $P_1(\mathbf{r};\mathbf{g}_1,\mathbf{g}_2)$ [Fig. 13(b)], and gather toward the center of $P_1(\mathbf{r};\mathbf{g}_1,\mathbf{g}_2)$, where the lowest minima of potential $V^l(r)$ exists. These movements result in the cross-shaped pattern seen in Fig. 13(c). Just before friction transition the pattern is connected by several atoms on the boundary line in $P_1(\mathbf{r};\mathbf{g}_1,\mathbf{g}_2)$. After friction transition, the pattern made by $P_1(\mathbf{r};\mathbf{g}_1,\mathbf{g}_2)$, is completely disconnected, as shown in Fig. 13(d) (cf. Fig. 6), thus confirming the validity of the friction transition criterion.

C. Friction transition for cubic metals

The main concern here is whether or not friction transition occurs in realistic frictional systems of several fcc and bcc metals. The Morse potentials determined by Girifalco and Wietzer[12] are used as the interatomic potentials of frictional systems. The friction transition calculation follows the same procedures as in the preceding

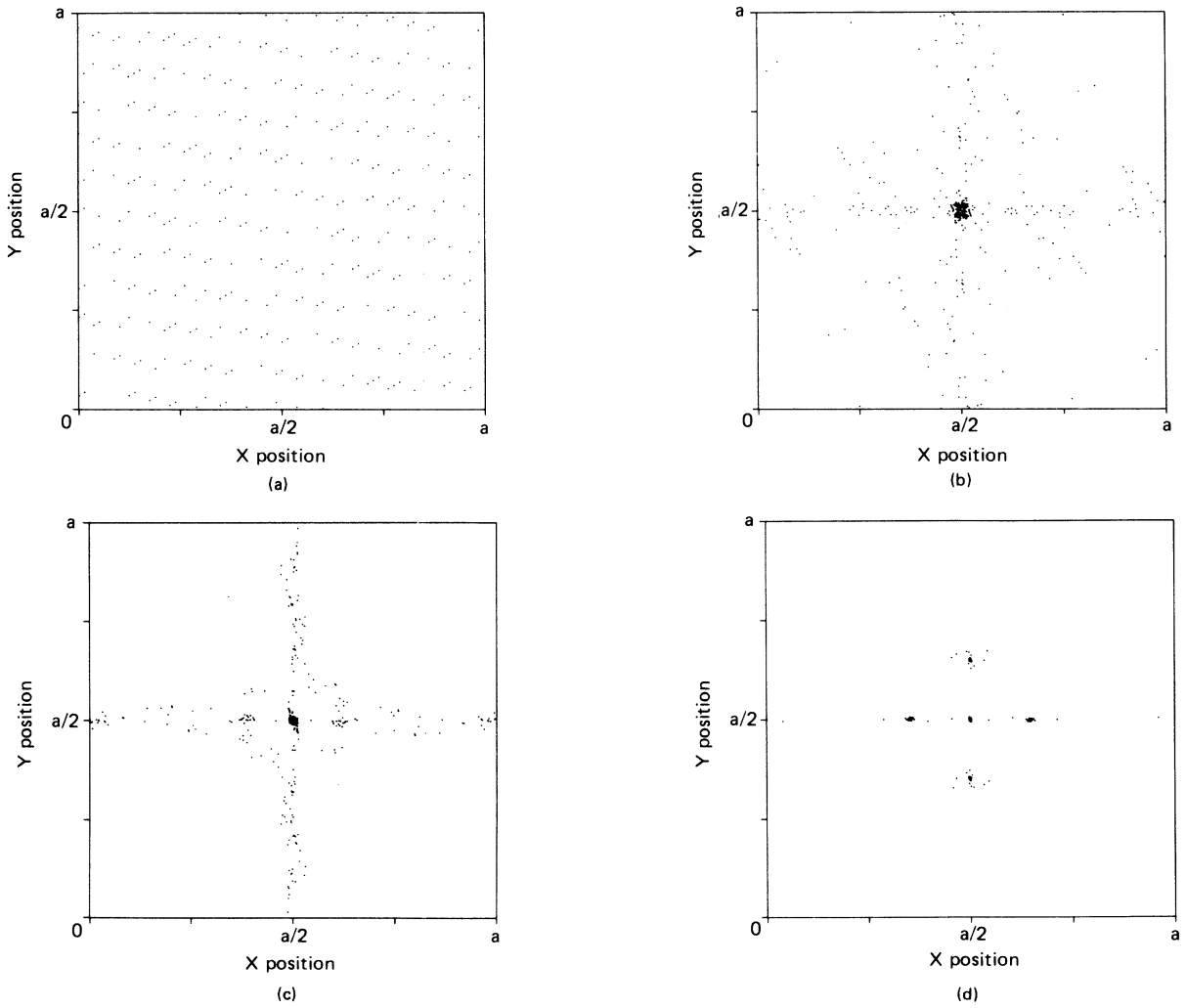

FIG. 13. Representative distributions $P_1(\mathbf{r};\mathbf{g}_1,\mathbf{g}_2)$. (a) shows distribution before relaxation. (b), (c), and (d) show distributions after relaxation when $D=10$, 20, and 60.

section. It is assumed that only the atoms of the upper body are allowed to change their positions while the atoms of the lower body remain fixed. To satisfy this assumption the closest packed crystal planes (hardest planes), such as the (111) planes for fcc lattices and the (110) planes for bcc lattices, are taken as the contact surfaces of the lower bodies. For fcc metals, planar atomic density increases with the $(110)<(001)<(111)$ planes. The (110) and (001) planes are then faced against the closest packed plane (111), as shown in Figs. 14(a) and 14(b). For the (110)-(111) contact, the upper body is composed of $(18\times12\times2)$ bct (body-centered tetragonal) unit cells (173 atoms) with unit vector $\mathbf{T}=(a/\sqrt{2},a,a/\sqrt{2})$ and the lower body is composed of $(29\times28\times2)$ monoclinic unit cells (5858 atoms) with unit vector $\mathbf{T}=(a/\sqrt{2},a/\sqrt{2},a/\sqrt{3})$. For the (001)-(111) contact, the upper body is composed of $(11\times11\times2)$ fcc units cells (1323 atoms) with unit vector $\mathbf{T}=(a,a,a)$ and the lower body is composed of the same monoclinic unit cells. For bcc metals, planar atomic density increases with the $(111)<(001)<(110)$ planes. The (001) and (111) planes are then faced against the closest packed plane (110), as shown in Figs. 14(c) and 14(d). For the (111)-(110) contact, the upper body is composed of $(18\times12\times2)$ monoclinic unit cells (1605 atoms) with unit vector $\mathbf{T}=(\sqrt{2}a,\sqrt{2}a,a/2\sqrt{3})$, and the lower body is composed of $(25\times25\times2)$ fct unit cells (6503 atoms) with unit vector $\mathbf{T}=(\sqrt{2}a,a,\sqrt{2}a)$. For the (001)-(110) contact, the upper body is composed of $(18\times12\times2)$ bcc unit cells (1173 atoms) with unit vector $\mathbf{T}=(a,a,a)$ and the lower body is composed of $(17\times23\times2)$ fct unit cells (4113 atoms) with unit vector $\mathbf{T}=(\sqrt{2}a,a,\sqrt{2}a)$. The critical atom for each contact is placed at the point satisfying $\partial V^l(r)/\partial r=0$ and $\partial^2 V^l(r)/\partial r^2<0$ along lines perpendicular to the ridge lines of $V^l(r)$, where the local minimum of potential $V^u(r_{\min})$ from the upper body and the local maximum of potential $V^l(r_{\max})$ from the lower body exists. In the calculation, the atoms of the upper body, excluding the criti-

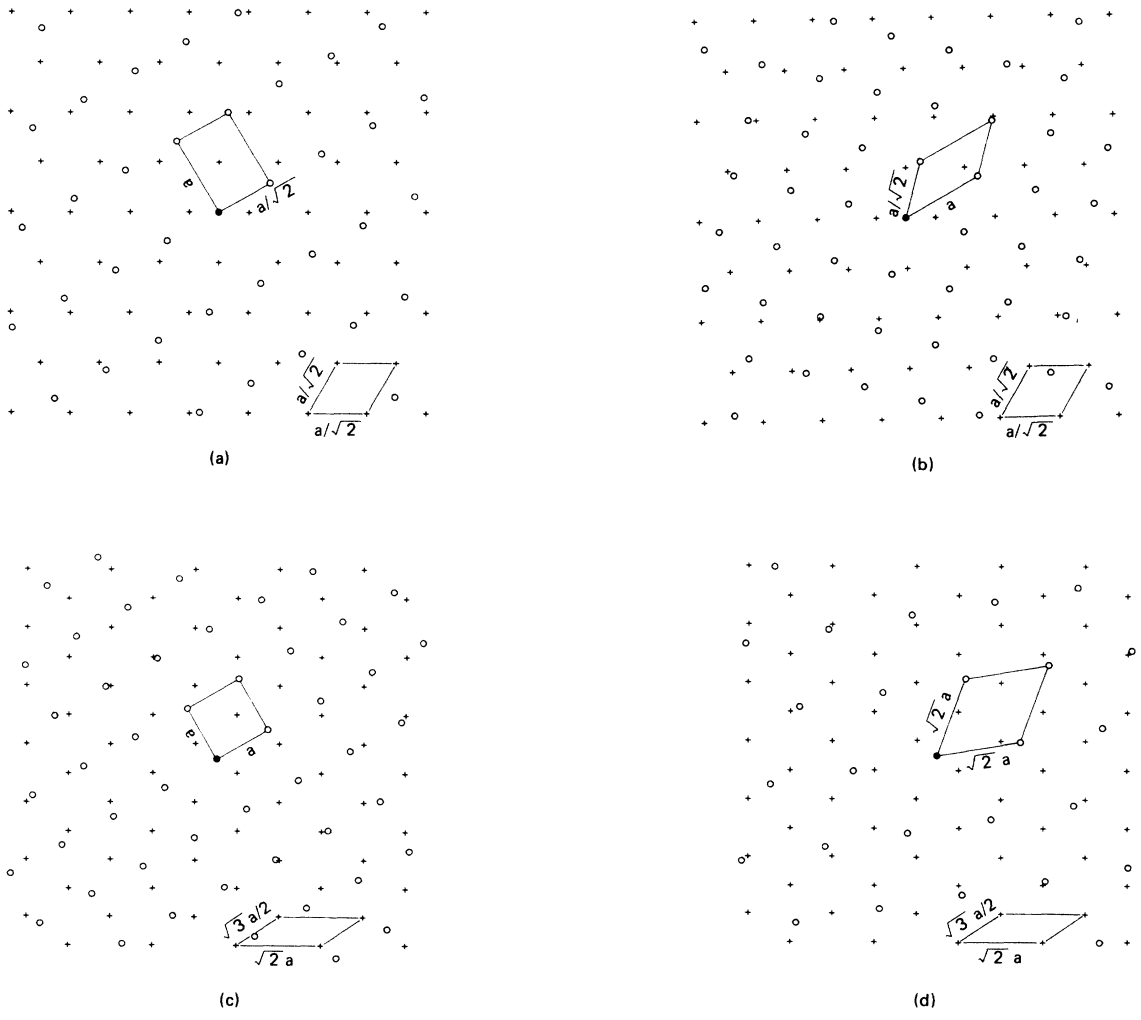

FIG. 14. Model for friction transition in realistic systems of cubic metals. For the fcc metals, a (110)-(111) contact (a) and a (001)–(111) contact (b) are examined. For the bcc metals, a (001)-(110) contact (c) and a (111)-(110) contact (d) are examined. The (○) symbols are upper-body atoms, and the (+) symbols are lower-body atoms. The (●) symbol is the critical atom.

cal atoms, are three-dimensionally relaxed. After relaxation second-order derivative $V_{\alpha,\beta}$ is calculated for the direction perpendicular to the ridge line of each critical atom.

Figure 15 shows the calculated $V_{\alpha,\beta}$ as a function of Morse potential parameter D. The calculated $V_{\alpha,\beta}$ values are positive for all of the examined metals. This shows that friction transition does not occur in these frictional systems. The $V_{\alpha,\beta}$ sign is actually determined by competition between a positive $V^u(r_{\min})$ contribution from the upper body and a negative $V^l(r_{\max})$ contribution from the lower body as seen in Eq. (4.17). A positive $V^u(r_{\min})$ always defeats a negative $V^l(r_{\max})$ in these frictional systems. Examining the value of $V_{\alpha,\beta}$ shows how much the frictional system is stable against friction transition. An increase in D increases the positive $V^u(r_{\min})$ contribution far more than the negative $V^l(r_{\min})$ contribution, thus giving a more positive $V_{\alpha,\beta}$ for the bcc metals than for the fcc ones.

It is also shown in Fig. 15 that $V_{\alpha,\beta}$ is dependent on the contact crystal plane. In bcc metals, for example, $V_{\alpha,\beta}$ for a (111)-(110) contact is larger than that for a (001)-(110) contact. How much $V_{\alpha,\beta}$ is dependent on the contacting crystal planes depends mainly on the differences between the positive $V^u(r_{\min})$ contributions of each contact. By separating mutual contribution U [see Eq. (4.4)], the atoms obtained from the bottom layer of the upper body for the total positive $V^u(r_{\min})$ contribution, the partial contribution of U, and its remainder in $V^u(r_{\min})$ can be selectively examined. Since the (111) plane in the bcc metals has less atomic density than the (001) plane, total $V_{\alpha,\beta}$ for the (111)-(110) contact is less than for the (001)-(110) contact before relaxation. However, the final $V_{\alpha,\beta}$ for the (111)-(110) contact is inversely larger than for the (001)-(110) contact after relaxation, resulting in a large increase in the positive contributions from the upper layers (2nd, 3rd, etc.) of the upper body by relaxation in the (111)-(110) contact. This is due to the fact that the atoms of the upper layers (2nd, 3rd, etc.) move toward the local lowest minima more easily in the (111)-(110) contact, since the (111) plane has less density. These situations also hold true for the fcc metals in the same way.

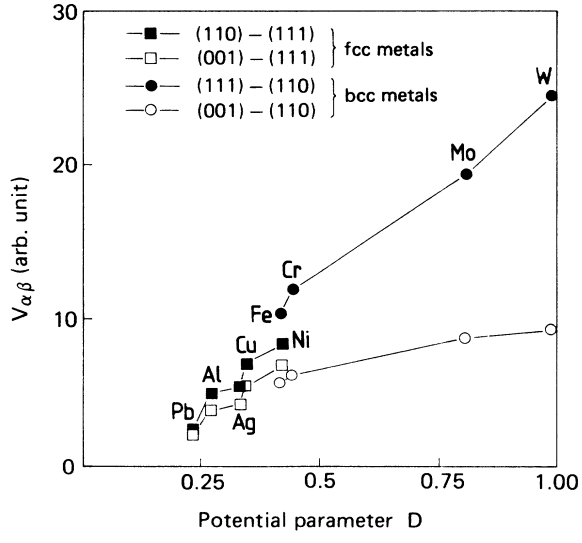

FIG. 15. Calculated $V_{\alpha,\beta}$ as a function of Morse potential parameter D.

VI. DISCUSSION AND CONCLUSION: ATOMIC LOCKING

Frictional properties were characterized by both the Q dependence of $P_1(\mathbf{r};\mathbf{g}_1,\mathbf{g}_2)$ and changes in the topological property of $P_1(\mathbf{r};\mathbf{g}_1,\mathbf{g}_2)$ that occurred due to the strength of interatomic potentials. The topological property of $P_1(\mathbf{r};\mathbf{g}_1,\mathbf{g}_2)$ is revealed in a pattern made by tiling $P_1(\mathbf{r};\mathbf{g}_1,\mathbf{g}_2)$ in a two-dimensional space. Frictional force vanishes when $P_1(\mathbf{r};\mathbf{g}_1,\mathbf{g}_2)$ is invariant with Q and its pattern is connected, but frictional force appears when $P_1(\mathbf{r};\mathbf{g}_1,\mathbf{g}_2)$ is variant with Q or the pattern is disconnected.

There are two atomistic origins for solid sliding friction: atomistic locking and dynamic locking. In atomistic locking, all the constituent atoms move continuously. Atomistic locking can occur for an arbitrary strength of potential $V^l(r)$. In the classical mechanical locking model, the (nonflat) potential surface that the upper body feels from the lower body spans on a large scale. In atomistic locking, the (nonflat) potential surface spans on an atomistic scale. On the other hand, in dynamic locking, the atoms discontinuously change their positions due to dynamic movements of the atoms. In contrast to atomistic locking, in dynamic locking the atoms nonadiabatically jump beyond potential barriers between neighboring sites. This origin cannot be described within the framework of the adiabatic potential. Dynamic locking follows disconnectedness of the connected pattern of a tiled $P_1(\mathbf{r};\mathbf{g}_1,\mathbf{g}_2)$ as $V^l(r)$ increases.

The criterion for the occurrence of friction transition was obtained. From studying the frictional properties of various systems, it can be concluded that friction transition may not appear for realistic systems, which suggests that atomistic locking is responsible for the solid sliding friction in these systems. The frictional force due to atomistic locking was calculated for α-iron. Average frictional force, as normalized by the contact area for a (001)-(001) contact of α-iron, is estimated to be 7.6 GPa. This frictional force will be comparable to the frictional force that is measured in future. Another important conclusion is that a frictionless system is apparently possible if clean solid surfaces are prepared. The performance of the experiments to confirm this possibility will be a highly desirable goal for the future.

A mechanism for solid friction similar to ours was proposed by Tomlinson.[17] He explained that the origin of solid sliding stems from dissipation of the elastic energy introduced by the relative sliding motion of two contacting solid bodies. This elastic energy is stored by an atom and is transformed into vibrational (or kinetic) energy, then is subsequently dissipated through the surrounding

atoms. The sum of the independently lost elastic energy stored by each atom is ascribed to the energy required to slide two contacting surfaces. His idea is different from ours, however, since he does not consider possible cooperative movements by the constituent atoms.

Further investigations on the dynamical properties of friction and frictional systems having noncrystalline surfaces, which has been experimentally observed for metals and ceramics, will be presented in the future.

ACKNOWLEDGMENTS

We gratefully acknowledge the stimulating discussions of Dr. R. Kaneko and Dr. K. Otuka. We also wish to thank Dr. T. Nakano for his interest in our study.

APPENDIX

The frictional properties are considered by taking mutal interaction U into account. The adiabatic potential is expressed with an approximation that neglects the higher-order terms rather than the second-order term of Δr_i^α:

$$W(\mathbf{Q})=\sum_i V^l(r_{i0}^1)+\sum_i V^u(r_{i,0}^1)+\sum_{i,j} V_{aa}(|\mathbf{r}_{i,0}^1-\mathbf{r}_{j,0}^1|)+\sum_{i,\alpha}\frac{\partial V^l(r_{i,0})}{r_{i,0}^\alpha}\Delta_i^\alpha+\tfrac{1}{2}\sum_{i,\alpha,\beta}[\epsilon_{i,j}(V_{i,j}^{l\alpha,\beta}+V_{i,j}^{u,\alpha,\beta})+U_{i,j}^{\alpha,\beta}]\Delta r_i^\alpha\Delta r_i^\beta \ . \tag{A1}$$

By using the orthogonal transformation

$$\Delta r_i^\alpha=\sum_{\mathbf{k}} c_{i;\mathbf{k},\lambda}q_{\mathbf{k},\lambda} \ , \tag{A2}$$

where

$$\sum_i c_{i;\mathbf{k},\lambda}^* c_{i;\mathbf{k}',\lambda'}=\delta_{\mathbf{k},\mathbf{k}'}\delta_{\lambda,\lambda'} \ , \tag{A3}$$

and

$$\sum_{\mathbf{k},\lambda} c_{i;\mathbf{k},\lambda}^* c_{j;\mathbf{k},\lambda}=\delta_{i,j} \ , \tag{A4}$$

which diagonalizes the last term on the right-hand side, giving

$$W(\mathbf{Q};\{q_{\mathbf{k},\lambda}\})=\sum_i V^l(r_{i0}^1)+\sum_i V^u(r_{i,0}^1)+\sum_{i,j} V_{aa}(|\mathbf{r}_{i,0}^1-\mathbf{r}_{j,0}^1|)+\sum_{\mathbf{k},\lambda}\gamma_{\mathbf{k},\lambda}+\tfrac{1}{2}\sum_{\mathbf{k},\lambda}\omega_{\mathbf{k},\lambda}q_{\mathbf{k},\lambda}^* q_{\mathbf{k},\lambda} \ , \tag{A5}$$

where $\gamma_{\mathbf{k},\lambda}$ is defined by

$$\gamma_{\mathbf{k},\lambda}=\sum_{i,\alpha}\frac{\partial V^l(r)}{\partial r_{i,0}^{1,\alpha}}c_{i;\mathbf{k},\lambda} \ . \tag{A6}$$

All eigenvalues $\omega_{\mathbf{k},\lambda}$ must be positive. When $V^l(r)=0$, displacement $q_{\mathbf{k},\lambda}=0$ from Eq. (A6). So, from Eq. (A2), $\Delta r_i^\alpha=0$ for all i and α. For a nonvanishing $V^l(r)$, the displacement is

$$q_{\mathbf{k},\lambda}=-\frac{\gamma_{\mathbf{k},\lambda}^*}{\omega_{\mathbf{k},\lambda}} \ , \tag{A7}$$

or

$$\Delta r_i^\alpha=-\sum_{\mathbf{k},\lambda}\frac{c_{i;\mathbf{k},\lambda}\gamma_{\mathbf{k},\lambda}^*}{\omega_{\mathbf{k},\lambda}} \ ,$$

$$\Delta r_i^\alpha=-\sum_{j,k,\lambda}\frac{c_{i;\mathbf{k},\lambda}\partial V(r)/\partial r_{j,0}^\alpha c_{j;\mathbf{k},\lambda}^*}{\omega_{\mathbf{k},\lambda}} \ . \tag{A8}$$

Below, the result in Eq. (4.12) is derived for a weak mutual interaction U. When $V^u(r)\gg U$, the dispersion of $\omega_{\mathbf{k},\lambda}$ is negligible. If $\omega_{\mathbf{k},\lambda}=\omega_0$ for all $\mathbf{k}$ in (A8), we have

$$\Delta r_i^\alpha=-\sum_{j,\mathbf{k},\lambda}\frac{c_{i;\mathbf{k},\lambda}\partial V(r)/\partial r_{j,0}^\alpha c_{j;\mathbf{k},\lambda}^*}{\omega_{\mathbf{k},\lambda}} \ ,$$

$$\Delta r_i^\alpha=-\frac{1}{\omega_0}\sum_{j,\mathbf{k},\lambda} c_{i;\mathbf{k},\lambda}\frac{\partial V(r)}{\partial r_{j,0}^\alpha}c_{j;\mathbf{k},\lambda}^* \ , \tag{A9}$$

by using the condition of normalization for $c_{i;\mathbf{k},\lambda}$ in (A2) and (A3),

$$\Delta r_i^\alpha=-\frac{1}{\omega_0}\sum_j\frac{\partial V(r)}{\partial r_{j,0}^{(\alpha)}} \ ,$$

$$\Delta r_i^\alpha=-\frac{1}{\omega_0}\frac{\partial V(r)}{\partial r_{i,0}^\alpha} \ . \tag{A10}$$

This completes the proof of Eq. (4.12).

Next the criterion for the friction transition is derived. The ridge lines of $V^l(r)$ correspond to the lines satisfying $\Delta r_i^\alpha=0$, or equivalently,

$$0=-\sum_{j,\mathbf{k},\lambda}\frac{c_{i;\mathbf{k},\lambda}\partial V(r_j)/\partial r_{j,0}^\alpha c_{j;\mathbf{k},\lambda}^*}{\omega_{\mathbf{k},\lambda}} \ . \tag{A11}$$

The criterion for the occurrence of friction transition is to see if the pattern obtained by tiling $P_1(\mathbf{r};\mathbf{g}_1,\mathbf{g}_2)$ is connected or disconnected along the ridge lines.

[1]The first scientific descriptions on frictional properties of materials appeared in the Italian Renaissance. Leonardo da Vinci studied solid sliding friction, and discovered the rules of sliding friction. For a review involving history in the field of friction see, e.g., N. Sota, *Masatu no Hanashi* (Iwanami Syoten, 1971) (in Japanese); D. Dowson, J. Lubr. Technol. Trans. ASME **99**, 383 (1978).

[2]C. A. Coulomb, Mémories de Mathematique et de Physics de l'Acaddemie Royale 161 (1978). For a review see, e.g., D. Tabor, J. Lubr. Technol. Trans. ASME **103**, 169 (1981); D. Dowson, *ibid.* **100**, 148 (1978).

[3]J. T. Desaguliers, *A Course of Experimental Philosophy,* Vol. 2; J. T. Desaguliers, Philos. Trans. R. Soc. London **33**, 345 (1725); D. Dowson, J. Lub. Technol. Trans. ASME **100**, 3 (1978).

[4]F. P. Bowden and D. Tabor, *Friction and Lubrication of Solids, Vol. II* (Clarendon, Oxford, 1964).

[5]R. Kaneko, K. Nonaka, and K. Yasuda, J. Vac. Sci. Technol A **6**, 291 (1988).

[6]C. M. Mate, G. M. McClelland, R. Erlandsson, and S. Chiang, Phys. Rev. Lett. **59**, 1942 (1987).

[7]G. Binnig, H. Rohrer, Ch. Gerber, and E. Weibel, Appl. Phys. Lett. **40**, 178 (1982); Phys. Rev. Lett. **49**, 57 (1982).

[8]See, e.g., V. I. Arnold and A. Avez, *Problémes Ergodiques de la Mécanique Classique* (Ganthier-Villas, Paris, 1967).

[9]S. Aubry, J. Phys. (Paris) **44**, 147 (1983).

[10]R. A. Johnson, Phys. Rev. **134**, 1329 (1964).

[11]H. M. Pak and M. Doyama, J. Fac. Eng. Univ. Tokyo B **30**, 111 (1969).

[12]Y. Waseda and S. Tamaki, J. Solid State Phys. (Japan) **1**, 133 (1976).

[13]L. A. Girifalco and V. G. Wezer, Phys. Rev. **114**, 687 (1959).

[14]R. Yamamoto, H. Matsuoka, and M. Doyama, Phys. Status Solidi A **51**, 163 (1979).

[15]A. T. Price, H. A. Holl, and A. P. Greenough, Acta Metall. **12**, 49 (1964).

[16]D. Tabor, Proc. R. Soc. London, Ser. A **251**, 1266 (1959); J. S. McFarlane and D. Tabor, *ibid.* A **202**, 1069 (1950).

[17]G. A. Tomlinson, Philos. Mag. **7**, 905 (1929).

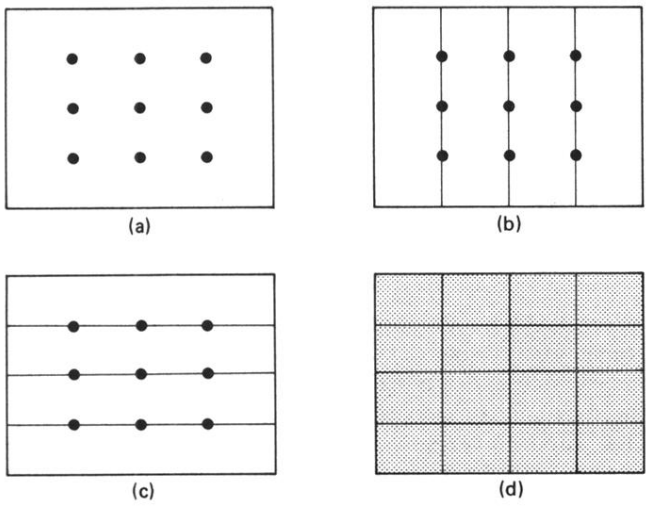

FIG. 2. Schematic illustrations of possible nonvanishing regions where the atoms of the upper body are projected onto a two-dimensional space spanned by g_1 and g_2 when $\bar{P}_\gamma(\boldsymbol{\rho})$ is variant with $\mathbf{Q}$. $[(\mathbf{g}_1',\mathbf{g}_1)/|\mathbf{g}_1|,\ (\mathbf{g}_2',\mathbf{g}_1)_i/|\mathbf{g}_1|,\ (\mathbf{g}_1',\mathbf{g}_2)_i/|\mathbf{g}_2|,\ (\mathbf{g}_2',\mathbf{g}_2)_i/|\mathbf{g}_2|)]=(r,r,r,r)$ for (a), (r,r,ir,r) or (r,r,r,ir) for (b) (r,ir,r,r) or (ir,r,r,r) for (c), and $(r,\mathrm{ir},r,\mathrm{ir})$ or $(\mathrm{ir},r,r,\mathrm{ir})$ or $(r,\mathrm{ir},\mathrm{ir},r)$ or $(\mathrm{ir},r,\mathrm{ir},r)$ for (d) where r represents rationality and ir irrationality.

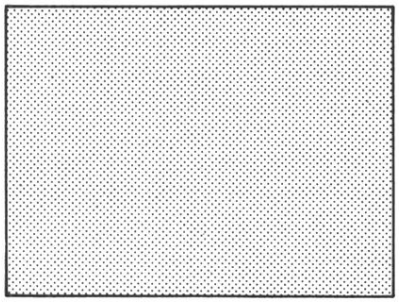

FIG. 3. Schematic illustrations of possible nonvanishing regions where the atoms of the upper body are projected onto a two-dimensional space spanned by g_1 and g_2 when $\bar{P}_\gamma(\boldsymbol{\rho})$ is invariant with $\mathbf{Q}$. $[(\mathbf{g}_1',\mathbf{g}_1)_i/|\mathbf{g}_1|,\ (\mathbf{g}_2',\mathbf{g}_1)_i/|\mathbf{g}_1|,\ (\mathbf{g}_1',\mathbf{g}_2)_i/|\mathbf{g}_2|,\ (\mathbf{g}_2',\mathbf{g}_2)_i/|\mathbf{g}_2|]=$(ir,ir,ir,ir), where ir represents irrationality.

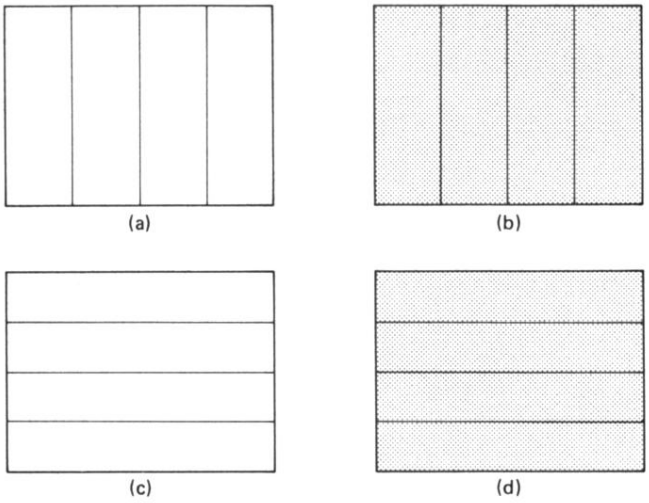

FIG. 4. Schematic illustrations of possible nonvanishing regions where the atoms of the upper body are projected onto a two-dimensional space spanned by g_1 and g_2 when $\overline{P}_\gamma(\boldsymbol{\rho})$ invariance with $\mathbf{Q}$ is restricted. $[(\mathbf{g}_1',\mathbf{g}_1)_i/|\mathbf{g}_1|,\ (\mathbf{g}_2',\mathbf{g}_1)_i/|\mathbf{g}_1|,\ (\mathbf{g}_1',\mathbf{g}_2)_i/|\mathbf{g}_2|,\ (\mathbf{g}_2',\mathbf{g}_2)_i/|\mathbf{g}_2|)]=(r,r,\mathrm{ir},\mathrm{ir})$ for (a) , $(r,\mathrm{ir},\mathrm{ir},\mathrm{ir})$ or $(\mathrm{ir},r,\mathrm{ir},\mathrm{ir})$ for (b), $(\mathrm{ir},\mathrm{ir},r,r)$ for (c), and $(\mathrm{ir},\mathrm{ir},\mathrm{ir},r)$ or $(\mathrm{ir},\mathrm{ir},r,\mathrm{ir})$ for (d), where r represents rationality and ir irrationality.

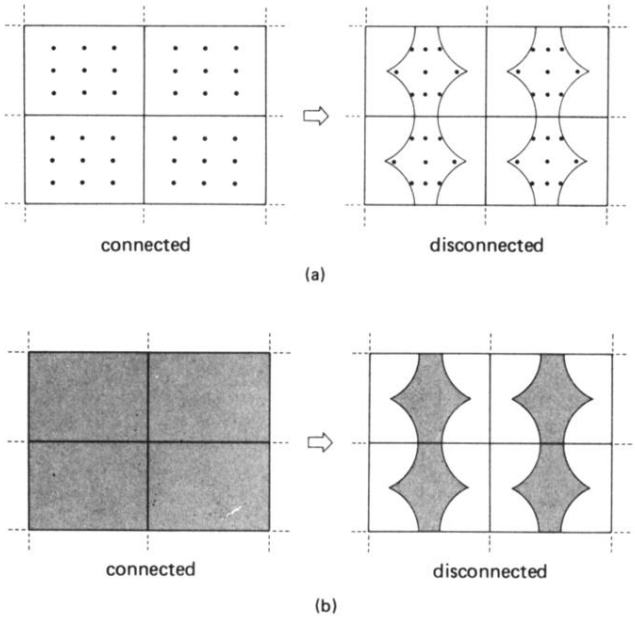

FIG. 6. Disconnectedness of a pattern made by tiling $P_1(\mathbf{r};\mathbf{g}_1,\mathbf{g}_2)$ periodically. (a) is the variant $P_1(\mathbf{r};\mathbf{g}_1,\mathbf{g}_2)$ case, and (b) is the invariant $P_1(\mathbf{r};\mathbf{g}_1,\mathbf{g}_2)$ case.